Liquid crystal-based square lens array with tunable focal length

Jiyoon Kim, Jonghyun Kim, Jun-Hee Na, Byoungho Lee, and Sin-Doo Lee*

School of Electrical Engineering, Seoul National University, Gwanak-Gu, Gwanakro 1, Seoul 151-744, South Korea
*sidlee@plaza.snu.ac.kr

Abstract: We demonstrate a liquid crystal (LC)-based square lens array with two focusing modes according to the polarization state of the input light. The homogeneously aligned LC layer is placed on an array of static square lenses fabricated using a photo-curable polymer whose refractive index is matched with the refractive index of the LC. For the input beam polarized parallel to the easy axis of the LC, the focal length is varied with the applied voltage from a few meters to 21 mm which corresponds to the focal length of the static lens. For the perpendicularly polarized input beam, the focal length is independent of the applied voltage and remains constant. The two focusing effects with high optical performance over fully activated areas are useful for polarization-dependent imaging systems and three-dimensional displays in projection and integral imaging.

©2014 Optical Society of America

OCIS codes: (250.0250) Optoelectronics; (220.3630) Lenses; (230.3720) Liquid-crystal devices.

References and links

1. L. Dong, A. K. Agarwal, D. J. Beebe, and H. Jiang, "Adaptive liquid microlenses activated by stimuli-responsive hydrogels," Nature **442**(7102), 551–554 (2006).
2. H. Ren and S.-T. Wu, "Tunable electronic lens using a gradient polymer network liquid crystal," Appl. Phys. Lett. **82**(1), 22–24 (2003).
3. H. Ren, J. R. Wu, Y.-H. Fan, Y.-H. Lin, and S.-T. Wu, "Hermaphroditic liquid-crystal microlens," Opt. Lett. **30**(4), 376–378 (2005).
4. H.-C. Lin and Y.-H. Lin, "An electrically tunable-focusing liquid crystal lens with a low voltage and simple electrodes," Opt. Express **20**(3), 2045–2052 (2012).
5. Y. Choi, H.-R. Kim, K.-H. Lee, Y.-M. Lee, and J.-H. Kim, "A liquid crystalline polymer microlens array with tunable focal intensity by the polarization control of a liquid crystal layer," Appl. Phys. Lett. **91**(22), 221113 (2007).
6. H. R. Stapert, S. del Valle, E. J. K. Verstegen, B. M. I. van der Zande, J. Lub, and S. Stallinga, "Photoreplicated anisotropic liquid-crystalline lenses for aberration control and dual-layer readout of optical discs," Adv. Funct. Mater. **13**(9), 732–738 (2003).
7. Y. Lu, Y. Yin, and Y. Xia, "A self-assembly approach to the fabrication of patterned, two-dimensional arrays of microlenses of organic polymers," Adv. Mater. **13**(1), 34–37 (2001).
8. C. H. Sow, A. A. Bettiol, Y. Y. G. Lee, F. C. Cheong, C. T. Lim, and F. Watt, "Multiple-spot optical tweezers created with microlens arrays fabricated by proton beam writing," Appl. Phys. B **78**(6), 705–709 (2004).
9. H. Ren, Y.-H. Fan, S. Gauza, and S.-T. Wu, "Tunable-focus flat liquid crystal spherical lens," Appl. Phys. Lett. **84**(23), 4789–4791 (2004).
10. W. Choi, D.-W. Kim, and S.-D. Lee, "Liquid crystal lens array with high-fill-factor fabricated by an imprinting technique," Mol. Cryst. Liq. Cryst. (Phila. Pa.) **508**, 35–40 (2009).
11. Y. Li and S.-T. Wu, "Polarization independent adaptive microlens with a blue-phase liquid crystal," Opt. Express **19**(9), 8045–8050 (2011).
12. Y.-H. Lin, H.-S. Chen, H.-C. Lin, Y.-S. Tsou, H.-K. Hsu, and W.-Y. Li, "Polarizer-free and fast response microlens arrays using polymer-stabilized blue phase liquid crystals," Appl. Phys. Lett. **96**(11), 113505 (2010).
13. C. J. Hsu and C. R. Sheu, "Using photopolymerization to achieve tunable liquid crystal lenses with coaxial bifocals," Opt. Express **20**(4), 4738–4746 (2012).
14. L. Lucchetti and J. Tasseva, "Optically recorded tunable microlenses based on dye-doped liquid crystal cells," Appl. Phys. Lett. **100**(18), 181111 (2012).
15. M. Hain, R. Glockner, S. Bhattacharya, D. Dias, S. Stankovic, and T. Tschudi, "Fast switching liquid crystal lenses for a dual focus digital versatile disc pickup," Opt. Commun. **188**(5–6), 291–299 (2001).
16. H. Ren, Y.-H. Fan, and S.-T. Wu, "Liquid-crystal microlens arrays using patterned polymer networks," Opt. Lett. **29**(14), 1608–1610 (2004).

#202868 - $15.00 USD Received 10 Dec 2013; revised 27 Jan 2014; accepted 28 Jan 2014; published 4 Feb 2014

17. H. T. Dai, Y. J. Liu, X. W. Sun, and D. Luo, "A negative-positive tunable liquid-crystal microlens array by printing," Opt. Express **17**(6), 4317–4323 (2009).
18. V. V. Presnyakov, K. E. Asatryan, T. V. Galstian, and A. Tork, "Polymer-stabilized liquid crystal for tunable microlens applications," Opt. Express **10**(17), 865–870 (2002).
19. J.-H. Na, S. C. Park, S.-U. Kim, Y. Choi, and S.-D. Lee, "Physical mechanism for flat-to-lenticular lens conversion in homogeneous liquid crystal cell with periodically undulated electrode," Opt. Express **20**(2), 864–869 (2012).
20. K. Asatryan, V. Presnyakov, A. Tork, A. Zohrabyan, A. Bagramyan, and T. Galstian, "Optical lens with electrically variable focus using an optically hidden dielectric structure," Opt. Express **18**(13), 13981–13992 (2010).
21. J.-H. Lee, H.-R. Kim, and S.-D. Lee, "Polarization-insensitive wavelength selection in an axially symmetric liquid-crystal Fabry-Perot filter," Appl. Phys. Lett. **75**(6), 859–861 (1999).
22. D.-W. Kim, C.-J. Yu, H.-R. Kim, S.-J. Kim, and S.-D. Lee, "Polarization-insensitive liquid crystal Fresnel lens of dynamic focusing in an orthogonal binary configuration," Appl. Phys. Lett. **88**(20), 203505 (2006).
23. J. Hong, Y. Kim, S.-G. Park, J.-H. Hong, S.-W. Min, S.-D. Lee, and B. Lee, "3D/2D convertible projection-type integral imaging using concave half mirror array," Opt. Express **18**(20), 20628–20637 (2010).
24. Y. Kim, K. Hong, J. Yeom, J. Hong, J.-H. Jung, Y. W. Lee, J.-H. Park, and B. Lee, "A frontal projection-type three-dimensional display," Opt. Express **20**(18), 20130–20138 (2012).
25. J. Kim, J.-H. Na, and S.-D. Lee, "Fully continuous liquid crystal diffraction grating with alternating semi-circular alignment by imprinting," Opt. Express **20**(3), 3034–3042 (2012).
26. Data sheet of ZLI-1800–100 provided by Merck, Ltd.
27. S.-T. Wu, "Birefringence dispersions of liquid crystals," Phys. Rev. A **33**(2), 1270–1274 (1986).

1. Introduction

Lens arrays are widely used for a variety of optical applications such as 3-dimensional displays [1–5], optical data storage devices [3–6], optical communication systems [5,7,8, and optical tweezers [4,8]. Among several types of lens arrays, liquid crystal (LC)-based lens arrays have been extensively studied due to the compactness, the easy fabrication, the high optical anisotropy, and the electrical tunability of the focal length at low voltages [4,9–14]. Since most of LC-based lens arrays were fabricated using patterned structures [5,9,10,15–17], patterned electrodes [13,15], polymer networks of the LCs [2,4,18] or surface relief structures [19], they suffered from the intrinsic drawbacks such as the limited aperture ratio and the low optical efficiency [2,9,10,13,20]. Basically, the LC is optically anisotropic and depends, in principle, on the polarization state of light. Such polarization dependence enables to design diverse optical devices including lens arrays for specific applications [5,17] but it often needs to be eliminated [21,22]. Regarding the focal length tunability of the LC-based lens arrays, both the convex lens effect and the concave lens effect were achieved depending on the difference between the ordinary and the extraordinary refractive indices of the LC [17]. Combined with the polarization dependence, the electrical tuning capability of the focal length of the LC lens array provides more sophisticated applications such as projection-type display systems and polarization dependent imaging systems [23,24]. However, no LC-based lens array having both the polarization-dependent focal length and the fully activated areas with high optical performance has been realized so far.

In this paper, we demonstrate a tunable LC-based square lens array with two focusing modes, one of which has a fixed focal length and the other a tunable focal length, over fully activated areas according to the polarization state of the input light. The refractive index of the static square lens, fabricated using a photo-curable polymer through an imprinting process, is matched with the extraordinary refractive index of the LC layer placed on the static lens. For the input beam polarized parallel to the easy axis of the LC in the homogeneous geometry, the focal length is varied with the applied voltage from a few meters to a static focal length (about 21 mm) while for the perpendicularly polarized input beam, the focal length is independent of the applied voltage and remains constant as in the static case. Note that our square lens array consists of the fully activated square areas with high uniformity and yields the polarization-dependent focal length which is electrically tunable at low voltages.

2. Concept of device configuration and operation principles

Figure 1(a) shows the schematic diagram of our LC-based square lens array. The bottom substrate was made of an indium-tin-oxide (ITO) coated glass on which transparent static

#202868 - $15.00 USD Received 10 Dec 2013; revised 27 Jan 2014; accepted 28 Jan 2014; published 4 Feb 2014
(C) 2014 OSA

lenses in square shape were fabricated using the ultraviolet (UV)-curable polymer by imprinting. The top substrate consists of the ITO coated glass and the LC alignment layer which was rubbed along the direction of the *y*-axis. As an optically anisotropic medium, an LC material was placed between the two substrates. Figure 1(b) and 1(c) show the operation principles when the polarization direction of the input light coincides with the easy axis of the LC (or the rubbing direction) and is perpendicular to it, respectively. It is clear that the incident light in Fig. 1(b) will not be refracted due to the index-match of the LC and the polymer material while the light in Fig. 1(c) will experience the refraction at the LC-polymer interface by the index difference. This results in the polarization-dependent focal length tuning capability by the applied voltage.

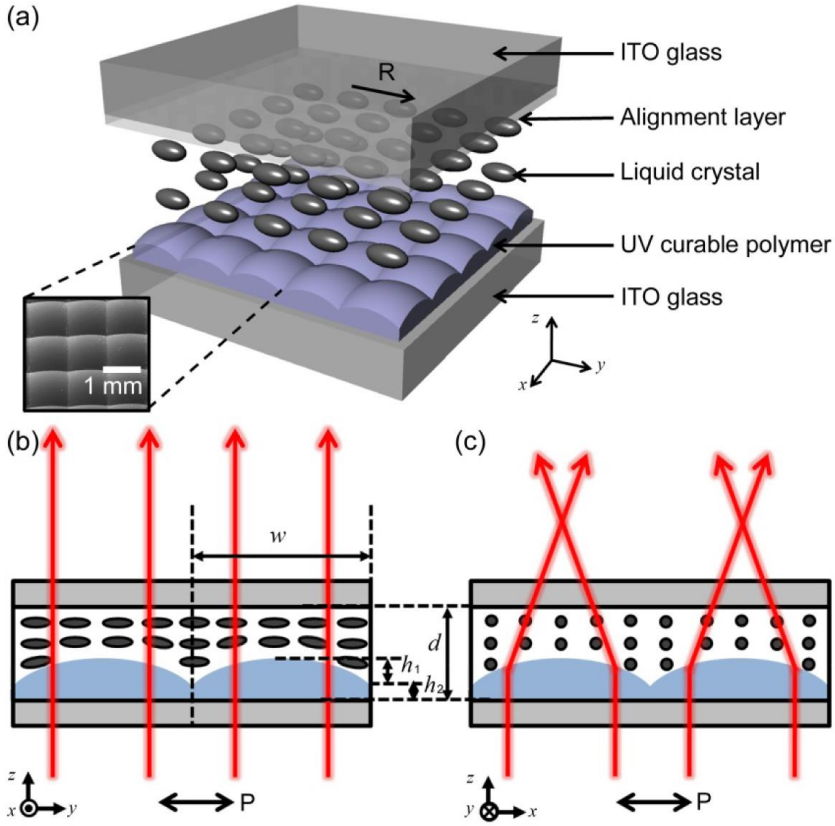

Fig. 1. (a) The schematic diagram of our LC-based square lens array (R denotes the rubbing direction of the top substrate). Operation principles when the polarization direction of the input light (b) coincides with the rubbing direction and (c) is perpendicular to the rubbing direction. Here, w, d, h_1, h_2 denote the length of the side of a square lens, the cell gap, the height of the lens part, and the height of the polymer background, respectively. The inset in (a) shows the SEM image of a portion the polymer lens array.

3. Experimental

A photo-curable polymer (NOA86, n = 1.55; Norland) was first prepared on an ITO coated glass by spin-coating at the rate of 1000 rpm for 20 s. The substrate was then imprinted with a master mold of the concave square lens array fabricated using poly(dimethylsiloxane) (PDMS; Sylgard-184, Dow Corning). For the master mold fabrication, the PDMS was poured on a template of a 1mm-convex lens array (FresnelTech), subsequently cured at 90 °C for 12 hours, and finally detached from the template. The imprinted substrate together with the master mold was exposed to UV light at the intensity of 100 mW/cm^2 for 1 min. The master

#202868 - $15.00 USD Received 10 Dec 2013; revised 27 Jan 2014; accepted 28 Jan 2014; published 4 Feb 2014
(C) 2014 OSA

mold was finally peeled-off. The length (w) of each side and the radius of curvature (R_c) of a single square lens were 1 and 1.62 mm, respectively. The inset in Fig. 1(a) is the scanning electron microscopic (SEM) image showing a portion of our square lens array made of the UV-curable polymer. The values of h_1 and h_2 were measured as 79.1 μm and 10 μm using a surface profiler (Alpha-step 200; KLA-TENCOR), respectively.

The homogeneous alignment layer of polyimide (RN-1199A; Nissan Chemical Industries, Ltd.) was prepared on the inner side of the top substrate in Fig. 1(a) by spin-coating at the rate of 3000 rpm for 30 s. The top substrate with the alignment layer was baked at 180 °C for 90 min and was unidirectionally rubbed. The bottom substrate and the top substrate were assembled such that the direction of the side of the square lens coincides with the rubbing direction. The thickness (d) of the LC cell was maintained using plastic spacers of 150 μm thick. A nematic LC (ZLI-1800-100, n_e = 1.5503, Δn = 0.0705; Merck) was finally injected into the LC cell by capillary action at room temperature. Note that since the UV-cured polymer produces the homogeneous alignment [5,25], the direction of the LC alignment on it (the bottom surface) is dictated by the rubbing direction on the other surface (the top surface) although it was not rubbed. The polarization state of the incident light on our LC-based square lens array was chosen to be either parallel or perpendicular to the rubbing axis.

4. Results and discussions

For our plano-convex type of the square lens consisting of a polymer and the LC, the focal length can be defined as $f = R_c/(n_p - n_{LC})$ in a simplified form. Here, f, n_p, n_{LC}, and R_c denote the focal length, the refractive index of the polymer, the refractive index of the LC, and the radius of curvature of the lens, respectively. In our case, R_c is 1.62 mm and n_p is about 1.55 which is matched with the refractive index of the LC, at the wavelength of 589 nm [26] in the range of the visible light. Note that the wavelength dispersion is rather small for low birefringence in the range of visible light [27]. When the polarization direction of the incident light is parallel to the easy axis of the LC, n_{LC} is simply n_e, and the focal length is then about 5400 mm. This means that the index-matched convex structure exhibits practically no lens effect at all this case. On the other hand, when the polarization direction of the incident light is perpendicular to the easy axis of the LC, n_{LC} becomes n_o, giving the focal length of about 23.1 mm. Such polarization dependence is confirmed from Fig. 2 where far-field images depending on the input polarization were shown. Figure 2(a) depicts the experimental geometry for capturing the far-field images at the distance of 200 mm (about 9 times longer than the static focal length of 23.1 mm) away from the lens array. Figures 2(b) and 2(c) show the far-field images observed when the polarization direction (P) of the illuminated light is parallel and perpendicular to the rubbing direction (R), respectively. As expected, no focusing effect was occurred in the case that the input polarization coincides with the rubbing direction as shown in Fig. 2(b).

Let us first examine the focusing effect of our square lens array as a function of the applied voltage with the help of a collimated laser beam at the wavelength of 543.5 nm in the focal plane as shown in Fig. 3(a). Figure 3(b) shows the CCD images captured under the applied voltages of 0, 4, 8, and 16 V when the polarization direction of the collimated beam is parallel to the rubbing direction in the LC-based square lens array. Clearly, the CCD images show the focusing effect. The intensity profiles of the images are shown in Fig. 3(b). At a relatively low voltage, the difference in the refractive index between the LC and the polymer is very small (about 0.0003) and no focusing effect appears. At a relatively high voltage of about 10 V (or the electric field of about 0.067 V/μm varying in the convex shape of the bottom substrate), the LC molecules become reoriented along the direction of the electric field (normal to the substrate) and the refractive index difference reaches at about 0.0702 which is sufficiently large to produce the focusing effect.

#202868 - $15.00 USD Received 10 Dec 2013; revised 27 Jan 2014; accepted 28 Jan 2014; published 4 Feb 2014
(C) 2014 OSA

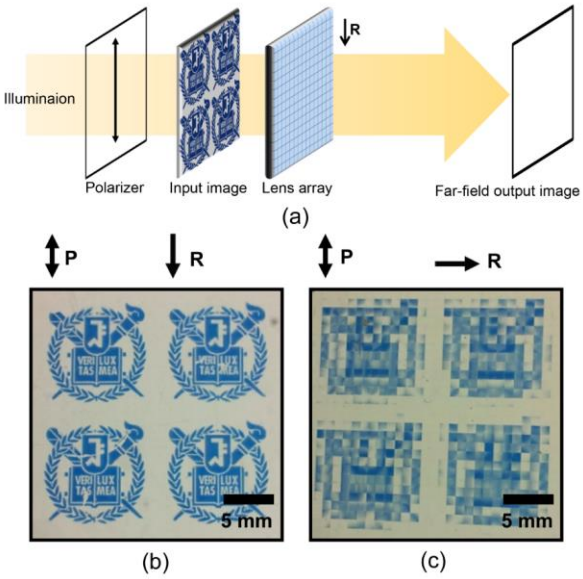

Fig. 2. (a) Experimental geometry for observing far-field output images through the lens array. Photographic images of our LC based square lens array with backlight polarized (b) parallel to the rubbing direction and (c) perpendicular to the rubbing direction. Here, P and R denote the optic axis of the polarizer and the rubbing direction on the top substrate, respectively.

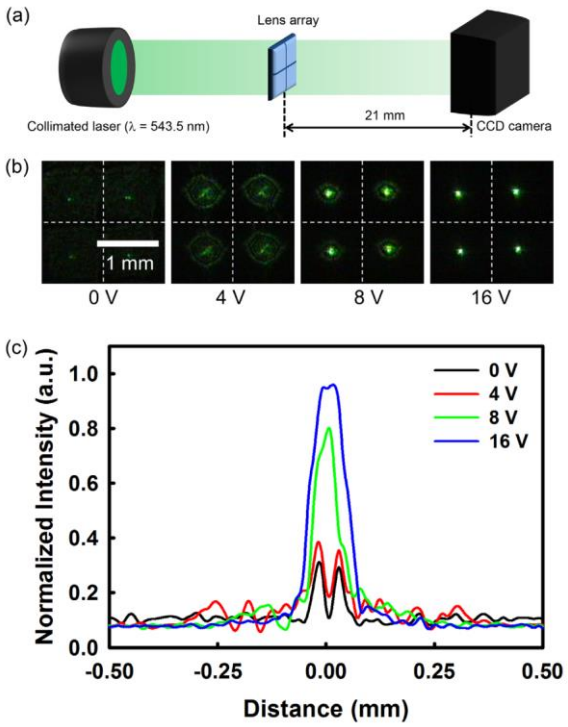

Fig. 3. (a) Experimental geometry for capturing a CCD image of a collimated laser beam in the focal plane of the lens array (2 X 2). (b) The images in the focal plane under the applied voltages of 0, 4, 8, and 16 V when the polarization direction of the input light was parallel to the rubbing direction. (c) The normalized intensity profiles under several different applied voltages when the polarization direction of the input light was parallel to the rubbing direction.

#202868 - $15.00 USD Received 10 Dec 2013; revised 27 Jan 2014; accepted 28 Jan 2014; published 4 Feb 2014
(C) 2014 OSA

The other case is shown in Fig. 4 where the polarization direction of the incident beam is perpendicular to the rubbing direction of the LC. It is clear from Figs. 4(a) and 4(b) that no focusing effect was essentially observed irrespective of the applied voltage, meaning that the focal length remains unchanged. In this case, the refractive index difference is simply 0.0702 regardless of the applied voltage.

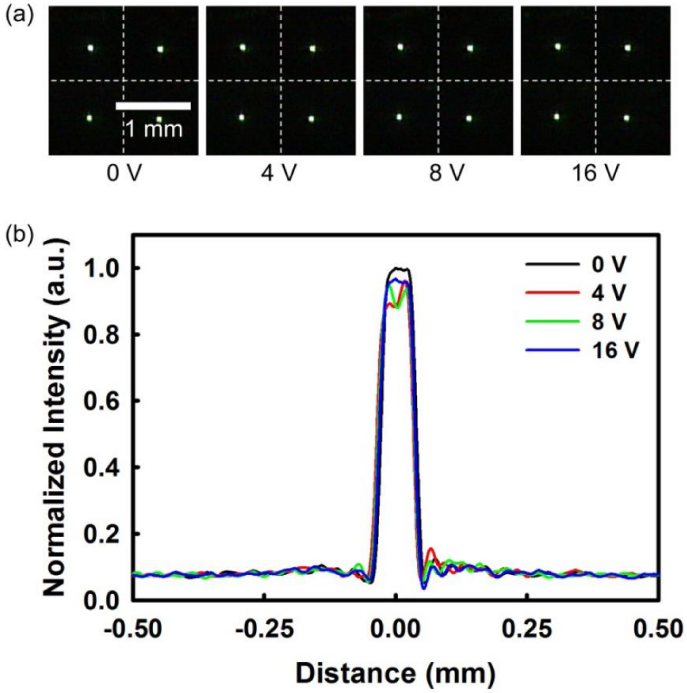

Fig. 4. (a) The CCD images of a collimated laser beam in the focal plane under the applied voltages of 0, 4, 8, and 16 V when the polarization direction of the input light was perpendicular to the rubbing direction. (b) The normalized intensity profiles under several different applied voltages when the polarization direction of the input light was perpendicular to the rubbing direction.

Figure 5 shows the focal length variations of our LC-based square lens array measured for the two cases as a function of the applied voltage. The focal length was varied from a few meters (about 120 mm at 2 V) to 21 mm in the high voltage limit. The focal length decreases with increasing the applied voltage due to the increase of the refractive index difference between the LC and the polymer when the polarization direction of the incident beam is parallel to the easy axis of LC. The measured focal length in the high voltage regime (about 21 mm) agrees well with the calculated value of 23.1 mm. The observed small difference may be attributed to the partial refraction occurred at the LC-polymer interface, the glass substrate-air interface, and some distortions of the LC director involved in the vicinity of the edge of the square lens. Under the applied voltage of 10 V, the rise time and fall time were about 1.2 s and 30 s, respectively. The response times are quite slow due to the thick cell gap inherent to the convex shape and the dimension of the lens in the bottom substrate. The LC lens configuration, the geometrical parameters such as the intrinsic curvature of each lens and the cell gap, and the materials remain to be optimized for relatively fast switching purposes.

#202868 - $15.00 USD Received 10 Dec 2013; revised 27 Jan 2014; accepted 28 Jan 2014; published 4 Feb 2014
(C) 2014 OSA

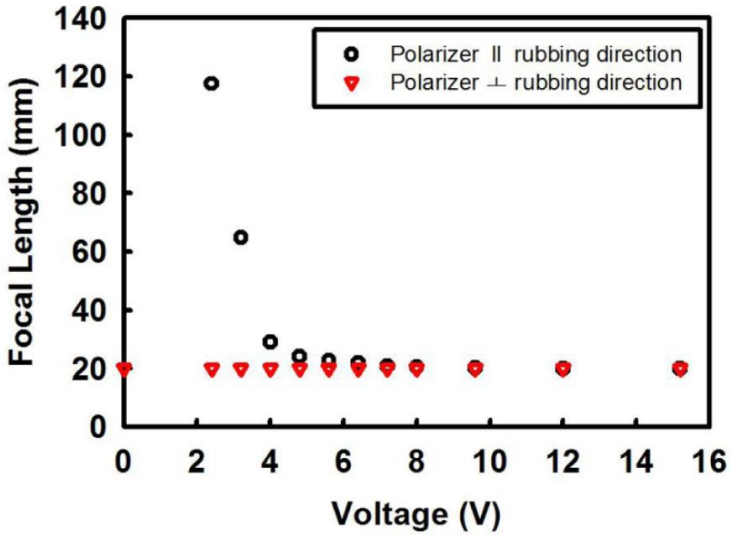

Fig. 5. The focal length of the square lens array as a function of the applied voltage.

We now describe the image selection capability of our LC-based square lens array depending on both the polarization state of the incident light with respect to the optic axis of the LC and the magnitude of the applied voltage. The experimental geometry for selecting certain focused images according to the polarization state and the applied voltage is shown in Fig. 6(a). Except for only a single square lens, all other surrounding lenses were blocked to eliminate any interference among them. The input image consists of 4 different characters of "M", "I", "P", and "D" arranged in two rows and two columns and located at the distance of 6 mm in front of the single square lens. The polarization states of the two columns are mutually orthogonal to each other as shown in Fig. 6(a). The output image focused in the real image plane was observed by the optical microscopy (Optiphot2-Pol; Nikon) at the distance of 10 mm from the square lens. Figures 6(b) and 6(c) show the output images when the rubbing direction is perpendicular to the polarization direction for the letters of "M" and "P" under the applied voltages of 0 V and 10 V, respectively. As expected, only the column having "I" and "D" was defocused and focused with varying the applied voltage. The output images when the angle (θ) between the rubbing direction and the polarization direction is θ = 45þ under the applied voltages of 0 V and 10 V are shown in Figs. 6(d) and 6(e), respectively. In this case, all the columns were defocused and focused by the applied voltage since two orthogonal polarization components exist. In the remaining case that the rubbing direction is parallel to the polarization direction for the letters of "M" and "P", the output images under the applied voltages of 0 V and 10 V are shown in Figs. 6(f) and 6(g), respectively. This is exactly opposite to what were observed in the first case. It is then concluded that the image selection over an entirely activated area can be performed using the LC-based square lens through a proper combination of the input polarization state and the applied voltage.

#202868 - $15.00 USD Received 10 Dec 2013; revised 27 Jan 2014; accepted 28 Jan 2014; published 4 Feb 2014
(C) 2014 OSA

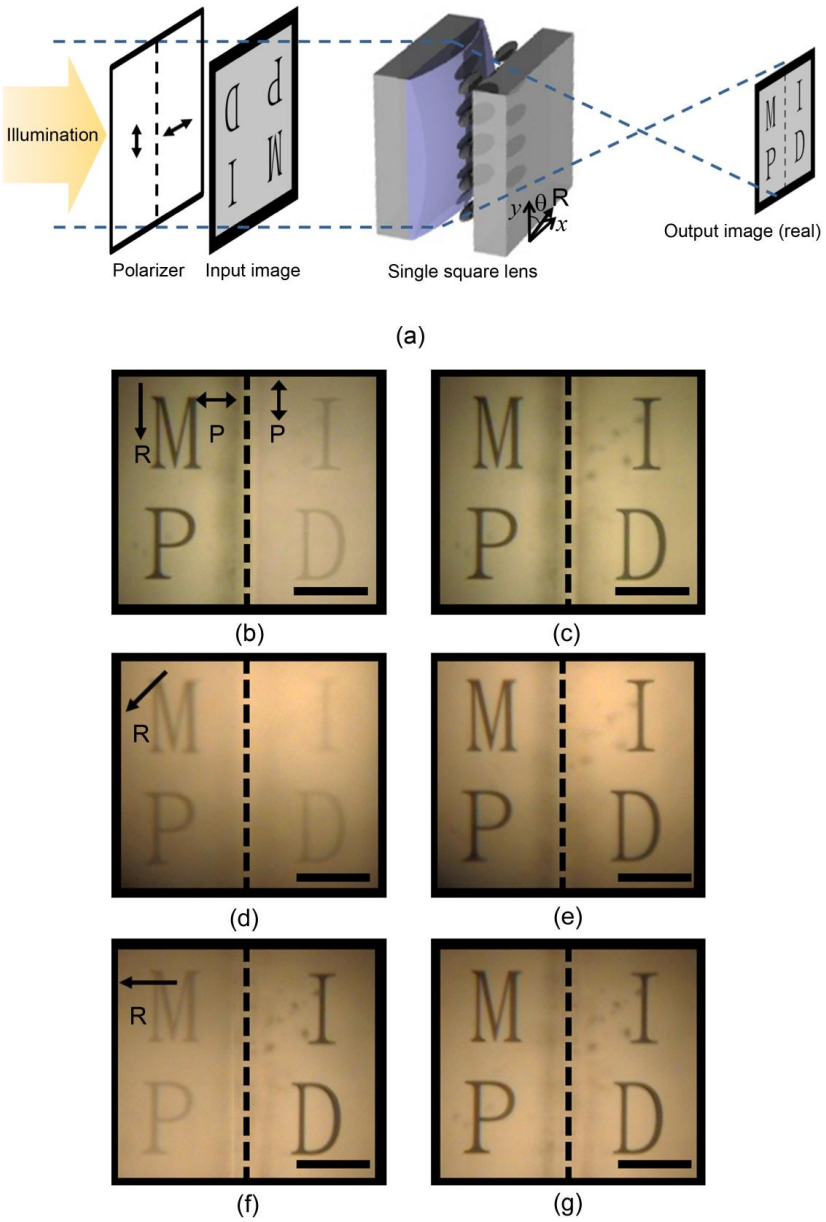

Fig. 6. (a) Experimental geometry for selecting certain focused images according to the polarization state and the applied voltages. The polarization direction for the letters of "M" and "P" and that for the letters of "I" and "D" were mutually orthogonal to each other. The output images when the rubbing direction was perpendicular to the polarization direction for the letters of "M" and "P" under the applied voltages of (b) 0 V and (c) 10 V. The output images when the angle θ between the rubbing direction and the polarization direction is 45þ under the applied voltages of (d) 0 V and (e) 10 V. The output images when the rubbing direction was parallel to the polarization direction for the letters of "M" and "P" under the applied voltages of (f) 0 V and (g) 10 V. The scale bar is 200 μm. Here, P and R denote the optic axis of the polarizers and the rubbing direction in the LC lens, respectively.

#202868 - $15.00 USD Received 10 Dec 2013; revised 27 Jan 2014; accepted 28 Jan 2014; published 4 Feb 2014
(C) 2014 OSA

5. Concluding remarks

We constructed an electrically LC-based square lens array with fully activated areas that exhibit two focusing modes with fixed and tunable focal lengths according to the polarization state of the incident light. There are two essential issues on the fabrication of such LC-based square lens array; one is the index-matching between the LC and the photo-curable polymer material. The other is to tailor the tuning range of the primary focal length in terms of the radius of curvature of an individual square lens. In our case, the focal length was varied from a few meters to 21 mm for the radius of curvature R_c ~1.62 mm, the refractive index of the polymer n_p ~1.55, and the birefringence of the LC Δn ~0.071. The tunable square lens array will be applicable for building up advanced imaging systems and displays requiring precise selection of the focused images in space by space according to the input polarization and the applied voltage.

Acknowledgment

This research was supported by Samsung Display, Co. Ltd.

#202868 - $15.00 USD Received 10 Dec 2013; revised 27 Jan 2014; accepted 28 Jan 2014; published 4 Feb 2014
(C) 2014 OSA

75.188.199.62 {ts '2018-03-30 23:44:57'}